

# Macromolecules

Volume 38, Number 19

September 20, 2005

© Copyright 2005 by the American Chemical Society

## Communications to the Editor

### Chemical Synthesis of Highly Conducting Polypyrrole Nanofiber Film

Aimei Wu, Harsha Kolla, and Sanjeev K. Manohar\*

Alan G. MacDiarmid Center for Innovation, Department of Chemistry, The University of Texas at Dallas, Richardson, Texas 75080

Received June 20, 2005

Revised Manuscript Received July 23, 2005

While polypyrrole having fibrillar morphology has been chemically synthesized using insoluble (hard) templates,<sup>1</sup> seeding,<sup>2</sup> and soluble (soft) templates such as large organic dopant anions having surfactant-like properties,<sup>3</sup> the use of conventional surfactants during the polymerization has largely yielded polypyrrole having particulate (nonfibrillar) morphology.<sup>4</sup> There are a few instances in which fibrillar morphology has been observed in surfactant-assisted polymerization of pyrrole.<sup>5</sup> In a recent report, nanowire/ribbonlike polypyrrole powder ( $\sigma_{RT} \sim 10^{-2}$  S/cm) was synthesized using the cationic surfactant cetyltrimethylammonium bromide (CTAB) under neutral aqueous conditions.<sup>6</sup> An insoluble lamellar precipitate of  $(CTA)_2S_2O_8$  is first formed which acts as a template for subsequent oxidative polymerization of the pyrrole present in the lamellar core. The lamellar structure is maintained as long as there is sufficient  $S_2O_8^{2-}$  in solution to replenish that which is consumed in the reaction; i.e., the mechanism requires excess peroxydisulfate to ensure fibrillar polymer growth ( $S_2O_8^{2-}/CTAB \sim 3$ ). The present study describes bulk nanofibrillar growth by leveraging different synthetic and mechanistic vectors: (i) the reaction is carried out in 1.0 M HCl, (ii) CTAB, HCl, and pyrrole combine to form a highly viscous network of threadlike micellar aggregates that act as templates for polymerization, and (iii) bulk polymerization takes place largely in the interior of these aggregates under a molar deficit of peroxydisulfate ( $S_2O_8^{2-}/CTAB < 0.5$ ). By simply filtering

the reaction mixture, a free-standing, nonwoven mat of highly conducting polypyrrole having nanofibrillar morphology can be readily isolated.

The synthetic procedure is outlined below. Pyrrole (0.13 M) was added to a cooled (0 °C), magnetically stirred solution of CTAB (0.1 M) in aqueous 1.0 M HCl (40 mL). The solution immediately turned very viscous. After vigorous stirring for 10 min, a solution of cooled (0 °C)  $(NH_4)_2S_2O_8$  (0.03 M) in aqueous 1.0 M HCl (40 mL), was added all at once, and the reaction mixture was stirred for 3 h at 0 °C. The resulting black precipitate of doped polypyrrole nanofibers was suction filtered in air and washed with copious amounts of deionized water and methanol. Air drying yielded a compact film on the surface of the filter paper that could be readily peeled off and cut using a blade.

The scanning electron microscopy (SEM) image of this film shows a nonwoven mat composed entirely of nanofibers of polypyrrole having diameter in the 20–40 nm range (Figure 1B). A robust free-standing film is obtained only when both CTAB and HCl are present in the reaction mixture. For example, no nanofibers are obtained in reactions carried out in deionized water with CTAB (Figure 1A) or in reactions carried out in aqueous 1.0 M HCl without CTAB (Figure 1C). The acid concentration also plays an important role; e.g., the 0.5 M HCl system yields only partially formed fibers (Figure 1D), while increasing the HCl concentration to 2.0 M results in much thicker fibers and/or flat ribbons (see Supporting Information). No nanofibers are obtained in 1.0 M  $H_2SO_4$ , suggesting that multivalent ions disfavor fibrillar polymer growth.

The polypyrrole film (CTAB/HCl system) is spectroscopically similar to polypyrrole nanofibers synthesized without CTAB, and elemental analyses show similar overall doping percentage for both systems (~18%). However, sulfate (not chloride) is the predominant dopant in the film which is consistent with higher local peroxydisulfate concentrations in systems containing CTAB (see below). The elemental analyses also show slightly elevated oxygen levels, which suggests its origin

\* Corresponding author: Fax (+1)972-883-6586; e-mail sanjeev.manohar@utdallas.edu.

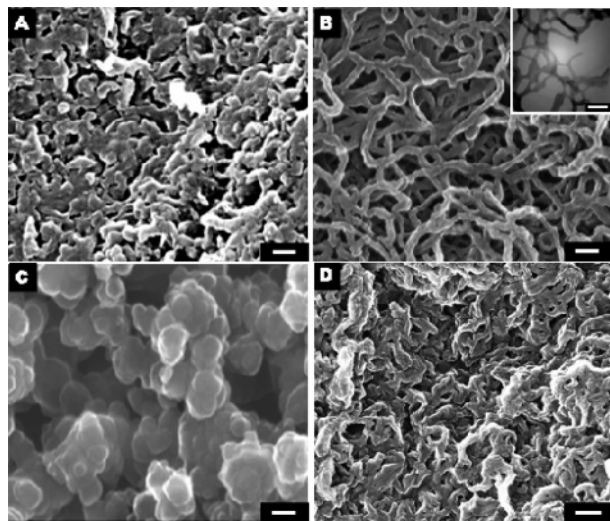


**Figure 1.** Scanning electron microscopy (SEM) images of doped polypyrrole synthesized using  $(\text{NH}_4)_2\text{S}_2\text{O}_8$  oxidant in (A) cetyltrimethylammonium bromide (CTAB)/deionized water, (B) CTAB/aqueous 1 M HCl, (C) aqueous 1 M HCl (no CTAB), and (D) CTAB/aqueous 0.5 M HCl. Inset in (B): TEM image of polypyrrole film. Scale: 100 nm.

**Table 1. Effect of Solution Microstructure on Polymer Morphology**

	$R_g^a$	$R_h^b$	cmc <sup>c</sup>	$\eta^d$	$\gamma^e$	morphology
CTAB/ $\text{H}_2\text{O}$		3.0	329	1	38	
CTAB/ $\text{H}_2\text{O}$ /pyrrole	18	3.7	233	8	35	particles
CTAB/HCl	22	4	14	1	36	
CTAB/HCl/pyrrole	37	15	5	640	32	fibers

<sup>a</sup> Radius of gyration (nm). <sup>b</sup> Hydrodynamic radius (nm). <sup>c</sup> Critical micelle concentration (ppm). <sup>d</sup> Viscosity (cP). <sup>e</sup> Surface tension (mN/m). <sup>f</sup> Cetyltrimethylammonium bromide.

to water of hydration or to water trapped inside the film. The four-probe conductivity of the free-standing film was  $\sim 50$  S/cm, which increased to  $\sim 100$  S/cm as a compressed pellet. To our knowledge, this is the first synthesis of a self-supporting free-standing film (nanofiber paper) of polypyrrole directly from pyrrole monomer. The film can be easily handled in air and cut into different shapes depending on end use.

The viscosity of the reaction mixture plays a key role in the evolution of fibrillar morphology. The viscosity of an aqueous 1.0 M HCl solution of CTAB increases dramatically when pyrrole monomer is added (Table 1), consistent with formation of a network of rodlike or threadlike micelles.<sup>7</sup> Both HCl and pyrrole are necessary; e.g., the viscosity of CTAB does not change significantly in aqueous 1.0 M HCl ( $\sim 1$  cP) although the critical micelle concentration (cmc) decreases from 329 to 14 ppm. However, upon addition of pyrrole, viscosity increases to 640 cP accompanied by a further drop in cmc to 5 ppm. Static and dynamic light scattering measurements provide additional information on the size of solution aggregates that are formed (Table 1); e.g., in the HCl system the hydrodynamic radius ( $R_h$ ) increases from 4 to 15 nm upon addition of pyrrole, whereas for the  $\text{H}_2\text{O}$  system this effect is significantly reduced. In this regard, the pyrrole system is different from our recently reported aniline system in which fibrillar morphology is favored in systems having higher cmc and surface tension.<sup>8</sup> These room temperature solution measurements have relevance at 0 °C (polymerization temperature) in view of the dramatic increase in solution viscosity and the potential role of micellar

aggregates as polymerization templates.<sup>7</sup> In addition, polypyrrole having nanofibrillar morphology is also obtained at room temperature.

The precise mechanisms associated with fibrillar polymer growth are unclear, although unlike the polyaniline system, it is much more difficult to obtain nanofibers of polypyrrole by chemical oxidative polymerization. The polymerization may be viewed temporally along the following lines: (i) the formation of large, relatively rigid micellar aggregates prior to addition of oxidant and (ii) evolution of fibrillar morphology upon addition of oxidant.

Prior to oxidant addition, pyrrole could be functioning as a pseudo-hydrotrope in CTAB solutions containing HCl.<sup>9</sup> The resulting increase in viscosity is qualitatively similar to CTAB/salicylate systems in which the salicylate carboxyl groups promote intermicellar bridges that help stabilize a highly viscous network of entangled micelles.<sup>7</sup> An analogue of this approach using oxalic CTAB/oxalic acid has been used to synthesize polyaniline nanofibers.<sup>10</sup> We believe the pyrrole/HCl system can help stabilize an analogous network of micellar aggregates via intermicellar hydrogen bonding. While the reduction in surface tension (and cmc) of CTAB by HCl/pyrrole is consistent with headgroup screening by increased ionic strength (HCl) and  $\pi$ -cation interactions between pyrrole and the positively charged headgroup at the palisade layer,<sup>11</sup> the viscosity increase points to longer range, cooperative interactions like a network of H-bonds. Unlike the CTAB/ $\text{H}_2\text{O}$  system, in which the pyrrole monomer is expected to be present predominantly at the micellar core, protonation by HCl is expected to drive pyrrole to the micellar interface in the CTAB/HCl system. The formation of these viscous micellar aggregates is likely a result of an interplay between increased acidity, which favors pyrrole migration to the exterior of the micellar core, and increased ionic strength, which helps drive the pyrrole to its interior.

Upon addition of oxidant, there would be an increase in the effective  $\text{S}_2\text{O}_8^{2-}$  concentration in the headgroup area due to electrostatic attraction. Whereas polymerization might be expected to be initiated at the outer palisade layer of the micellar aggregate, we believe bulk polymerization takes place in the micellar core. Evidence consistent with this rationale is obtained from elemental analysis where the majority dopant is  $\text{HSO}_4^-$  (12%) compared to  $\text{Cl}^-$  (5.7%) even though the reaction is carried out in 1.0 M HCl. In contrast,  $\text{Cl}^-$  is the predominant dopant in the absence of CTAB. Additionally, when pyrrole is displaced from the micellar core by the more hydrophobic cyclohexane (added just prior to addition of oxidant), only polypyrrole having particulate morphology is obtained (see Supporting Information).

The experimental evidence is also not consistent with the reaction taking place via the intermediacy of a lamellar precipitate of  $(\text{CTA})_2\text{S}_2\text{O}_8$ .<sup>6</sup> For example, we also observe a white precipitate of  $(\text{CTA})_2\text{S}_2\text{O}_8$  in our CTAB/ $\text{H}_2\text{O}$  system, but in view of our low  $\text{S}_2\text{O}_8^{2-}$ /CTAB molar ratio (0.3), no fibrillar morphology is observed, which is consistent with the lamellar mechanism outlined previously. In contrast, the CTAB/HCl system yields fibrillar polypyrrole despite the low  $\text{S}_2\text{O}_8$ /CTAB molar ratio, pointing to a fundamentally different mechanistic pathway (micellar) that we believe could be leveraged to advantage in the synthesis of a variety

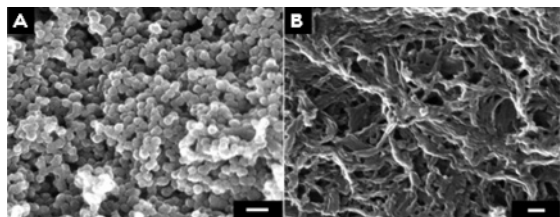


**Figure 2.** Scanning electron microscopy (SEM) images of polypyrrole synthesized using cetyltrimethylammonium bromide and  $\text{FeCl}_3$  oxidant in (A) deionized water and (B) aqueous 1 M HCl. Scale: 100 nm.

of polymeric systems. In addition, when  $\text{FeCl}_3$  is used as the oxidant, polypyrrole having fibrillar morphology is obtained (Figure 2B). Since no CTAB- $\text{FeCl}_3$  precipitate is formed under these conditions,<sup>6</sup> solution microstructure, e.g., threadlike or rodlike micellar aggregates, could be playing an important role in orchestrating fibrillar polymer growth in both oxidant systems.

In summary, we demonstrate (i) a simple mix-and-filter aqueous method to synthesize, in one step, free-standing films of highly conducting polypyrrole composed entirely of nanofibers (20–40 nm diameter) and (ii) a highly viscous CTAB/HCl/pyrrole system that provides a semirigid framework (template) for fibrillar polymer growth.

**Acknowledgment.** We gratefully acknowledge helpful discussions with Professor Alan G. MacDiarmid and The University of Texas at Dallas for financial support.

**Supporting Information Available:** Tables of elemental analyses of polypyrrole in HCl and DI water systems; SEM

images of doped polypyrrole and digital image of free-standing polypyrrole nanofiber film. This material is available free of charge via the Internet at <http://pubs.acs.org>.

## References and Notes

- (1) Ikegame, M.; Tajima, K.; Aida, T. *Angew. Chem., Int. Ed.* **2003**, *42*, 2154–2157. Martin, C. R. *Science* **1994**, *266*, 1961–1966.
- (2) Zhang, X.; Manohar, S. K. *J. Am. Chem. Soc.* **2004**, *126*, 12714–12715.
- (3) Long, Y.; Zhang, L.; Chen, Z.; Huang, K.; Yang, Y.; Xiao, H.; Wan, M.; Jin, A.; Gu, C. *Phys. Rev. B* **2005**, *71*, 165412/165411–165412/165417. Yang, Y.; Liu, J.; Wan, M. *Nanotechnology* **2002**, *13*, 771–773.
- (4) Carswell, A. D. W.; O'Rear, E. A.; Grady, B. P. *J. Am. Chem. Soc.* **2003**, *125*, 14793–14800. Omastova, M.; Trchova, M.; Kovarova, J.; Stejskal, J. *Synth. Met.* **2003**, *138*, 447–455.
- (5) He, C.; Yang, C.; Li, Y. *Synth. Met.* **2003**, *139*, 539–545. Jang, J.; Yoon, H. *Chem. Commun.* **2003**, 720–721.
- (6) Zhang, X.; Zhang, J.; Liu, Z.; Robinson, C. *Chem. Commun.* **2004**, 1852–1853.
- (7) Manohar, C.; Rao, U. R. K.; Valaulikar, B. S.; Iyer, R. M. *J. Chem. Soc., Chem. Commun.* **1986**, 379–381. Pokhriyal, N. K.; Joshi, J. V.; Goyal, P. S. *Colloids Surf.* **2003**, *218*, 201–212.
- (8) Zhang, X.; Manohar, S. K. *Chem. Commun.* **2004**, *20*, 2360–2361.
- (9) Fu, H.; Xiao, D.; Yao, J.; Yang, G. *Angew. Chem., Int. Ed.* **2003**, *42*, 2883–2886. Goyal, P. S.; Aswal, V. K. *Curr. Sci.* **2001**, *80*, 972–979.
- (10) Zhong, W.; Deng, J.; Yang, Y.; Yang, W. *Macromol. Rapid Commun.* **2005**, *26*, 395–400.
- (11) Currie, F. *J. Colloid Interface Sci.* **2004**, *277*, 230–234.

MA051299E